

A Thesis

entitled

Development of Induced Magnetic Field Procedure for Nondestructive Evaluation of
Deteriorated Prestressing Strand

by

Michael D. Titus

Submitted to the Graduate Faculty as partial fulfillment of the requirements for the
Master of Science Degree in Civil Engineering

Dr. Douglas Nims, Committee Chair

Dr. Vijay Devabhaktuni, Committee Member

Dr. Brian Randolph, Committee Member

Dr. Patricia R. Komuniecki, Dean
College of Graduate Studies

The University of Toledo
May 2011

Copyright 2011, Michael Dennes Titus

This document is copyright material. Under copyright law, no parts of this document may be reproduced without the expressed permission of the author.

An Abstract of

Development and Field Test of Induced Magnetic Field Procedure for
Nondestructive Evaluation of Deteriorated Prestressing Strand

by

Michael D. Titus

Submitted to the Graduate Faculty as partial fulfillment of the requirements for the
Master of Science Degree in Civil Engineering

The induced magnetic field (IMF) procedure for nondestructive evaluation of deteriorated prestressing strand predicts the sound cross-sectional area of strand in embedded concrete. The system utilizes an electromagnet that magnetizes the strand, and an array of hall sensors that measures Gauss readings that indicate the strength of the magnetic field of the strand. This technology allows bridge inspectors to go further than visual inspection when determining the condition of prestressed concrete beams. This thesis discusses the development of the IMF testing system, including both laboratory testing and a field test. During the course of this research, the magnetic flux leakage (MFL) testing procedure was also researched and utilized. The first documented field test of its kind was performed using magnetic inspection on a prestressed box beam bridge. The IMF system accurately predicted corrosion in a laboratory setting, and predicted corrosion during the field test, albeit with limited accuracy. The MFL method predicted corrosion more accurately in the field test.

Acknowledgements

The author would like to thank Dr. Douglas Nims, Dr. Vijay Devabhaktuni, Bertrand Fernandes, and James Wade for their work towards developing the IMF testing system. I would also like to thank my thesis committee members, including Dr. Nims, Dr. Devabhaktuni, and Dr. Brian Randolph, for their time, thoughtful input, and assistance. The Ohio Department of Transportation and the Fayette County Engineer provided funding and the bridge for the field test which was critical to the research. I also appreciate the donations of strand by Nucor and RettCo Steel which made the laboratory testing possible. Lastly, I would like to thank my family and friends for their support and motivation during my college career.

Contents

Abstract.....	iii
Acknowledgements.....	iv
List of Tables	vii
List of Figures.....	viii
1 Introduction.....	1
1.1 Overview.....	3
1.2 Problem Statement.....	3
1.3 Research Objectives.....	4
2 Literature Review.....	5
2.1 Lehigh University Study – “Inspection Methods & Techniques to Determine Non Visible Corrosion of Prestressing Strands in Concrete Bridge Components”.....	5
2.2 Magnetic Flux Leakage.....	6
2.3 Difference between Induced Magnetic Field and Magnetic Flux Leakage	8
3 Laboratory Experiments.....	9
3.1 Sample concrete beams.....	9
3.2 Wooden Beam Test.....	14
3.2.1 Wooden Beam - Test Procedure	15

4	Field Test	21
4.1	Magnetic Flux Leakage Test Setup.....	23
4.2	Field Test Platform	23
4.3	Basic Field Test Procedure	25
4.4	Induced Magnetic Field Test Details and Results.....	26
4.5	Magnetic Flux Leakage Test Details and Results.....	30
4.5.1	Interior Beams.....	31
4.5.2	Exterior Beam.....	34
4.6	Dissection and Results Comparison.....	36
5	Bridge Inspection.....	41
5.1	Inspection Recommendations	41
5.2	Maintenance and Repair	43
6	Conclusions and Future Work	45
6.1	Conclusions.....	45
6.2	Improvements and Future Work	46
	References.....	48
	Appendices.....	51
	Appendix A.....	51
	Appendix B.....	54
	Appendix C.....	55

List of Tables

Table 3.1:	3/8" diameter strand, various cover and various water level in concrete.	12
Table 3.2:	Scan data for 4-strands and 3-strand arrangement.	20
Table 4.1:	Corrosion estimated for Tracks 3I and 7I from IMF method.	30
Table 4.2:	Results obtained from dissection of bridge compared with MFL and IMF estimated corrosion results over entire scan length.	40
Table 5.1:	Strength of corroded strand.	42

List of Figures

3-1:	Small scale concrete beam (3/8" Strand).....	10
3-2:	Small scale concrete beam (PVC sleeves).....	10
3-3:	Wood test beam.	15
3-4:	Right pole face sensor layout. Note: Sensor 1 is in same position as Sensor 2 but on the opposite pole face.	17
3-5:	Wooden beam, 3/8" strand spaced 1.75" C/C, #4 stirrups at 15" C/C.....	17
4-1:	Cross section of Washington Waterloo Rd Bridge box girder (Wagner, circa 1967).	22
4-2:	Testing platform attached to bottom of bridge.	24
4-3:	IMF sensing equipment, electromagnet with hall sensors on pole face.	26
4-4:	MFL sensing equipment.	26
4-5:	3/8" Strand with concrete gaps.....	28
4-6:	IMF scan data for interior beams – Tracks 3I and 7I.	29
4-7:	MFL scan data for interior beams – Tracks 1I, 3I, 7I and 10I.	33
4-8:	MFL scan data for exterior beams – Tracks 1E, 3E, and 4E.....	35
4-9:	Cut strand cross-section (in.) (Track 3I – Dissection Area 2).	36
4-10:	Results for corrosion detected for interior and exterior tracks by MFL method – reflected plan.....	37
4-11:	Dissection results of Area 2 in interior beam 3.	38

5-1: Inspection flowchart, longitudinal crack patterns. Data from (Naito, et al. 2010).	42
5-2: Corrosion levels on strand (Naito, et. al, 2010).....	43

Chapter 1

Introduction

Prestressing strands embedded in concrete are susceptible to corrosion that leads to a reduction in strength of the concrete members. Prestressed box beams are commonly used for bridge construction. Roughly 10% of bridges in Ohio are prestressed box beam bridges (Nims, 2010), and about one-sixth of the bridges constructed annually across the nation are of this type (Russell, 2011). When used for bridge construction, prestressed box beams are subject to water, salt, and freeze/thaw cycles. These factors can lead to corrosion of the embedded strands that cannot be seen with visual inspection. A research team from Lehigh University (Naito, 2010) has developed guidelines that improve the accuracy of visual inspection based upon cracks. While this provides good practical information for bridge inspectors, the need to more accurately predict hidden corrosion in bridge box beams exists. In 2005, a prestressed box bridge beam collapsed in Pennsylvania. Upon inspection following the collapse, corrosion was found in the embedded strands that were not visible prior to collapse. A nondestructive evaluation technique which could identify corrosion in these members earlier and more accurately would be valuable to bridge inspectors, Department of Transportation (DOT) officials, and public safety.

The University of Toledo, more specifically Dr. Douglas Nims, Dr. Vijay Devabhaktuni, Mr. James Wade, and Mr. Bertrand Fernandes have developed a magnetic testing system which determines the cross-sectional area of steel. Proof of concept testing was completed on a system for magnetic in-situ detection of prestressing strand cross-sectional area (Wade, 2010). Detailed explanations of the design and principles behind this induced magnetic field (IMF) testing system can be found in their research documents (Fernandes, 2010). The goals of this research were to further develop the testing system and perform a field test of the system on a bridge to be demolished. The field test was a valuable tool in identifying areas of improvement of the system. In addition to field testing the University of Toledo's IMF system, Dr. Ghorbanpoor from the University of Wisconsin-Milwaukee was contracted to perform the same testing using his magnetic test system, magnetic flux leakage (MFL). The MFL system has been identified by the *ATLSS Report No. 09-09*, "Inspection methods & techniques to determine non visible corrosion of prestressing strands in concrete bridge components, Task 2 – Assessment of candidate NDT methods", (Jones, et al., 2010), as successful in predicting corrosion in a laboratory setting in a comprehensive evaluation of nondestructive bridge inspection techniques. The report was published during the course of this research and obtained valuable information related to the IMF development. The report confirmed what early work in developing this system had discovered, magnetic type inspection techniques are the most successful in determining corrosion in embedded strand.

1.1 Overview

The IMF system utilizes an electromagnet with a magnetic field value of 194 ampere/centimeter (A/cm) with an array of hall sensors that measure the induced magnetic field of the magnetized strand. The value of 194 A/cm is important because it was determined in the initial design phase that a magnetic field of that strength is needed to obtain sufficient magnetic saturation of the prestressing strand typically found in concrete bridges. The system was designed by James Wade and Bertrand Fernandes of the University of Toledo and a more detailed technical explanation of the IMF system can be found in their research documents (Wade, 2010 and Fernandes, 2010). An explanation of how strand area is calculated is included later in this thesis.

1.2 Problem Statement

Corrosion can occur of the embedded prestressing strand that is found in concrete beams. Covered by concrete, this corrosion can go unnoticed. A cost effective nondestructive evaluation (NDE) technique for determining corrosion in embedded prestressing strands would be beneficial to bridge inspectors and DOT officials. Currently, visual inspection is used to determine the condition of prestressed box beam, but in many cases, strand may be corroding beneath the concrete invisible to the naked eye. IMF aims to solve this problem by providing inspectors with an estimate of the cross-sectional area of the embedded strand using a non-evasive test procedure. This information can then be used to assess the condition of the beams and ultimately, load rate the bridge.

1.3 Research Objectives

The goal of this research is to advance the state of IMF technology to make it viable for bridge inspection. Performing this will help to deliver to the Ohio Department of Transportation (ODOT) a method for inspection of prestressed box beams. To work towards these goals, lab testing and a field test were performed which helped understand the testing process and determine the practicality of using the system in the field setting. Feasibility issues were uncovered during the course of the field test that will be discussed later in this paper.

Chapter 2

Literature Review

The prevalence of corrosion in embedded steel in concrete structures has led to a variety of strategies towards determining corrosion levels. Methods such as acoustic emission monitoring, ultrasonic defect detection, ground penetrating radar (Ciolko, A. T. and Tabatabai, H., 1999) and magnetic methods like magnetic flux leakage (MFL) (Ghorbanpoor et al., 2000) and remnant magnetic field (RMF) methods have been applied (Scheel and Hillemeier, 1997; 2003; Hillemeier and Scheel, 1998). Among these, magnetic methods have been successfully used in determining hidden corrosion in embedded strand in prestressed concrete. They have successfully identified various corrosion levels related to loss of section or fractures in prestressing strands (Jones et al., 2010; Naito and Jones, 2010).

2.1 Lehigh University Study – “Inspection Methods & Techniques to Determine Non Visible Corrosion of Prestressing Strands in Concrete Bridge Components”

Researchers at Lehigh University recently conducted a three part study on “Inspection Methods & Techniques to Determine Non Visible Corrosion of Prestressing

Strands in Concrete Bridge Components” spurred by the collapse of a box beam bridge over I-70 near Pittsburgh, Pennsylvania in 2005. The bridge beam collapsed due to its own dead load. The three tasks in the study were a “Literature Review”, an “Assessment of Candidate NDT Methods”, and “Forensic Evaluation and Rating Methodology”. The literature review is a comprehensive resource of published literature related to corrosion of prestressing strands in pre-tensioned bridge applications. The “Assessment of Candidate NDT Methods” is a study of six nondestructive testing methods, including two magnetic methods for determining corrosion and fractures in prestressing strands. The “Forensic Evaluation and Rating Methodology” discusses how cracking patterns can help reveal the location of corrosion and presents new recommendations for inspecting and rating box beams. More details on their inspection recommendations can be found in their work and later in this thesis in the “Bridge Inspection” section. The assessment of the Non Destructive Testing (NDT) methods presented MFL as the most accurate in predicting corrosion and flaws in prestressing strand (Jones, 2010). This led the research team at The University of Toledo to contact Dr. Al Ghorbanpoor from the University of Wisconsin-Milwaukee about his MFL system.

2.2 Magnetic Flux Leakage

Magnetic methods have been used routinely for inspections of wire ropes and other cables in air (ASTM E1571, Fernandes, 2010). Magnetic flux leakage has been used for damage detection applications in pipelines (Chen et al., 2005) and flat surfaces, to detect inner and outer defects (Mihalache et al., 2000). The MFL method was introduced by Kusenberger (Kusenberger and Barton, 1981) for investigating steel in

prestressed concrete members. This method was extended to facilitate its use on site (Sawade and Krause, 2007; Ghorbanpoor, 1998a,b). Using the MFL technique, researchers at the University of Nebraska, (DaSilva et al., 2009) used permanent magnets to create a magnetic field around corroded strands to detect corrosion.

The MFL method is a magneto-static measurement technique. When an external magnetic field is applied to reinforced or prestressed concrete members, the flux within the reinforcing or prestressing steel remains unchanged until it must leave the steel to travel back to the opposite pole of the second magnet. If the flux encounters a flaw such as a corroded area, broken strand, or complete fracture, some or all of the flux leaks out of the steel. This magnetic flux leakage is detected by one or more sensors and is analyzed to determine the extent or severity of the discontinuity (Edwards, 1999). These leaks are detectable by visual inspection of the graphs obtained from the scan. A trained eye is required to identify the flaws and corrosion found in these graphs, which is performed by comparing the graphical results to previous known results. The magnitude of the detected MFL signal depends on the distance between the sensor and the prestressing steel. The induced magnetic field strength should be adequately large to cause considerable magnetic flux leakage to occur when there are small defects in the steel. As a result, if sufficient magnetic saturation of the strands is not provided, flaws smaller than a few percent of the cross-sectional area may not be detected using the MFL. This magnetic saturation is dependent upon the strength of the magnets utilized, the size of the strand to magnetized, and the distance between the two.

The MFL method has been used on site for more than a decade to inspect prestressed tendons. In every case, measured corrosion or rupture signals have been

confirmed to originate from “tendon corrosion or cracks” by visual inspection after opening the concrete (Ghorbanpoor, 2000). This has also been validated by the studies at Lehigh University previously discussed (Jones et al., 2010). Among the various techniques analyzed and tested, the magnetic methods were able to provide the most accurate and reliable predictions of different damage levels due to corrosion and fractures. It was shown that the accuracy of the MFL method was better than the RMF method at identifying flaws in both conventional steel reinforced concrete and 7-wire reinforced concrete slab specimens.

2.3 Difference between Induced Magnetic Field and Magnetic Flux Leakage

The procedure for determining corrosion using the induced magnetic field method developed by Wade and Fernandes involves saturating the strand and measuring the field produced. The difference in magnetic field can be correlated with lab data to determine if a reduction in Gauss has occurred in a scan width, detected by the hall sensors positioned on the electromagnets’ pole face. If a reduction is found, an amount of corrosion can be determined. Alternatively, MFL is based upon detecting flux that leaks from the strand when flaws are present. MFL is more quantitative in detecting corrosion, but because it is only interested in the detection of flaws, it can utilize lighter less powerful magnets.

Chapter 3

Laboratory Experiments

Two main laboratory tests were performed with the IMF test system. The first “sample concrete beams” occurred prior to the field test, while “wooden beam test” was conducted after the field test. There are many factors that affect the readings obtained from the Hall sensors used to determine Gauss readings. These include the cross-sectional area of the strands within the effective sensor width, the distance from the sensor to the strand (unknown when the strand is embedded), the strand pattern itself (center-to center spacing, stirrup spacing, etc.), water present during the scan, and the effect of concrete on the magnetic waves. Lab tests were performed to address each of these factors and determine how they affect the magnetic readings.

3.1 Sample concrete beams

Two small scale concrete beams were utilized to test the IMF system (see Figures 3-1 and 3-2). There were multiple items to learn with these laboratory tests. The test was set up so that multiple readings could be obtained as the concrete cured. The purpose behind this was to identify if water would have an effect on the readings obtained during the scan process. In many instances, water has been found inside

concrete box beams. To determine the effect of water, the same areas were tested 2, 7, and 30 days after the concrete was poured. While an IMF scan would not normally be performed this early in a beams life cycle, this allowed for measurements with a variable amount of water in the concrete.



Figure 3-1: Small scale concrete beam (3/8" Strand).



Figure 3-2: Small scale concrete beam (PVC sleeves).

There was also experimentation to determine the best location for the hall sensors and way to obtain readings to get consistent results. The beams were constructed with four strands in a box like pattern with the purpose of determining the effect of adjacent strands on the magnetic readings. Each of the four sides had different cover distances from the face of the concrete to the location of the strand. Lastly, one beam was constructed with 3/8" strand, a size commonly used in bridges of this kind built in the 1960s-1970s (see Figure 3-1). Another beam was constructed with PVC pipes in place of the strand (see Figure 3-2). The reasoning behind this was to allow for various sizes of strand to be inserted into the beam. PVC was selected because it would not affect the magnetic readings. The results of the experiment are in Table 3.1.

Table 3.1: 3/8" diameter strand, various cover and various water level in concrete.

1" Concrete Cover

Days after pour	Dia.	Area (in ²)	Sensor Reading (G)	Change from prior scan (G)	Position of strands relative to magnet
2	3/8"	0.085	1650	N/A	Strand centered over magnet face
7	3/8"	0.085	1710	60	Strand centered over magnet face
30	3/8"	0.085	1677	-33	Strand centered over magnet face
2	3/8"	0.085	1870	N/A	Pair of strands centered over magnet face
7	3/8"	0.085	1800	-70	Pair of strands centered over magnet face
30	3/8"	0.085	1660	-140	Pair of strands centered over magnet face

1 1/4" Concrete Cover

Days after pour	Dia.	Area (in ²)	Sensor Reading (G)	Change from prior scan (G)	Position of strands relative to magnet
2	3/8"	0.085	1560	N/A	Strand centered over magnet face
7	3/8"	0.085	1590	30	Strand centered over magnet face
30	3/8"	0.085	1570	-20	Strand centered over magnet face
2	3/8"	0.085	1610	N/A	Pair of strands centered over magnet face
7	3/8"	0.085	1600	-10	Pair of strands centered over magnet face
30	3/8"	0.085	1547	-53	Pair of strands centered over magnet face

1 3/4" Concrete Cover

Days after pour	Dia.	Area (in ²)	Sensor Reading (G)	Change from prior scan (G)	Position of strands relative to magnet
2	3/8"	0.085	1460	N/A	Strand centered over magnet face
7	3/8"	0.085	1420	-40	Strand centered over magnet face
30	3/8"	0.085	1410	-10	Strand centered over magnet face
2	3/8"	0.085	1450	N/A	Pair of strands centered over magnet face
7	3/8"	0.085	1430	-20	Pair of strands centered over magnet face
30	3/8"	0.085	1447	17	Pair of strands centered over magnet face

The tests show that there is a slight correlation with the amounts of water in the concrete surrounding the strands. The column, “Change from prior scan”, shows the difference of gauss from the previous reading (i.e. the difference of Day 30 from Day 7), hence the change in reading as less water is in the concrete from the curing process. In six out of eight of the readings from seven and 30 days after the pour, the gauss readings were less than the previous. In most cases though, there was very little difference, but certain instances saw large changes. The largest gaps were 53 and 40 gauss, which could make a difference in the amount of steel predicted. The average difference of all the tests was 13.25 gauss, which would translate into a difference in area of steel predicted of a few percent. In most cases of a field inspection there would be very little water to affect the test. This data shows that when water is present during the test the readings may be affected, but not significantly. However, it was difficult to obtain consistent readings for the magnetic flux. If water in the concrete becomes a concern in future testing, more laboratory testing utilizing an automated test system, similar to the system later in this section, should be performed.

The effect of adjacent strands was not immediately clear during the test, later laboratory tests helped to understand the situation in more detail. These tests showed, in general, when the two strands are positioned over the magnet face (and the hall sensor positioned in between the two strands on the center of the magnet face) higher results are obtained. The test setup did not provide enough information to accurately assess the true affect adjacent strands had on the results. The wooden beam test conducted later in the research process determined that different strand patterns have a large effect. Therefore, before testing a beam it is important to identify the strand pattern used during

construction and perform tests on a mock-up beam that would recreate a 100% cross-sectional area scenario. More on the testing process will be discussed later.

This test was performed with a handheld LakeShore 410 Gaussmeter, which made it extremely difficult to obtain readings at the exact same location on the pole face. Different positions on the pole face have different magnetic strengths. To account for the difficulties in obtaining consistent readings, each measurement was taken three times and averaged. Following this test, all subsequent tests performed used hall sensors attached to the pole face surface. Attaching the hall sensors directly to the face takes out the variable of sensor position. With the updated setup, readings are collected using an Optim MEGADAC and laptop, which also increases the testing rate.

3.2 Wooden Beam Test

Following the “sample concrete beam” test a field test was performed, which is discussed later. After completion of the field test, to be described in Chapter 4, it was determined more laboratory testing was necessary to become more familiar with the test process and to improve the efficiency of the scanning. Previous experiments determined concrete has minimal effect on the magnetic flux readings. This allowed for a mock beam made of wood to be constructed to further test the IMF system. The wooden beam was constructed so that the strands could be moved into multiple configurations (see Figure 3-3). One of the key difficulties in the field test was testing the underside surface of the bridge. The wooden beam was constructed so that the IMF sensing system could be rolled along the ground with the beam positioned directly above the electromagnet pole faces/sensors.



Figure 3-3: Wood test beam.

3.2.1 Wooden Beam - Test Procedure

In order to more accurately assess the cross-sectional area of steel within a scan width a new test procedure was created. The new procedure was created because some variables affect magnetic reading more than first thought, such as the strand and stirrup pattern. This procedure involves the following steps:

1. Attach hall sensors to pole face (see Figure 3-4).
2. Obtain readings from each hall sensor with magnet on and no steel in detectable range of the magnet. This value will be used as the baseline minimum reading for the magnet.
 - a. This step is performed because it has been noticed that various positions on the face of the magnet have different magnetic strengths. Environmental factors, such as temperature can also affect

electromagnetic strength. To ensure accurate results, this step should be performed once before a test session.

3. Perform a scan of the strand layout to be tested, using known healthy strand (see Figure 3-5). This value represents a 100% strand area.
 - a. This scan should be performed using a layout as close to the actual beam design as possible, using details such as cover, center to center spacing, stirrup spacing, and strand diameter.
4. Perform a scan of the unknown test specimen. It is important that this scan is performed at the same distance from pole face to strand as the scan in Step 3. The value obtained is the test scan value.
5. The following equation is then performed for each sensor; % area of steel for sensor width = $(\text{test scan value} - \text{baseline value}) / (100\% \text{ strand area value} - \text{baseline value})$. Step 5 should be completed for each sensor (four sensors in the case of this set of experiments).
 - a. This percentage obtained gives the percentage of cross-sectional area of strand remaining within that sensor's effective scan width.
6. The values obtained from Step 5 for each sensor should then be averaged. This average value is the percentage area of healthy strand remaining in the scan width (6 in.).



Figure 3-4: Right pole face sensor layout. Note: Sensor 1 is in same position as Sensor 2 but on the opposite pole face.

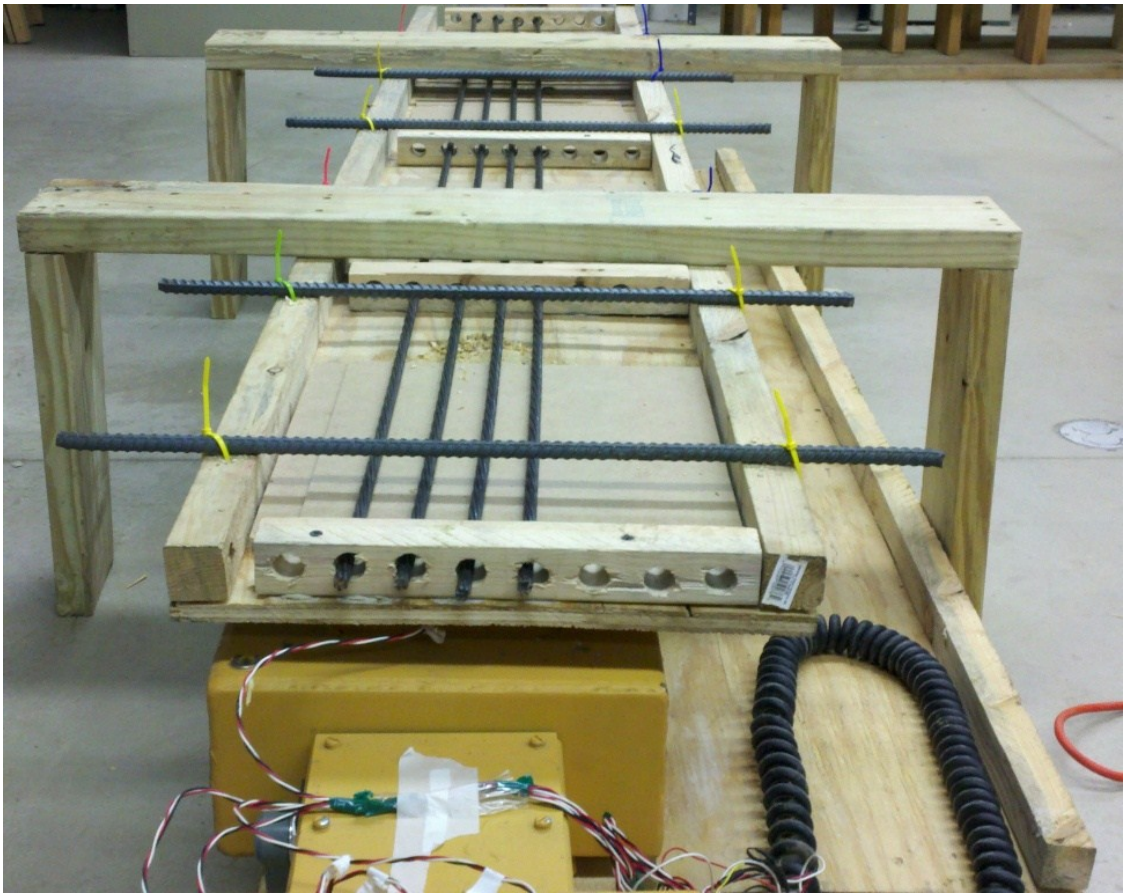


Figure 3-5: Wooden beam, 3/8" strand spaced 1.75" C/C, #4 stirrups at 15" C/C.

In order to validate the new test procedure, the following experiments were performed. Four 3/8" strand were tested to obtain the value for 100% strand area. One strand was then removed and the scan was performed again. The three strands were then rearranged and different variations of strand patterns were tested. The strands were then reduced to two out of four, and then one out of four until multiple variations were completed to determine the accuracy of the test procedure. Results were within +/- 7% of the expected results each time. To obtain accurate results the electromagnet must be turned off more than 50% of the time. If the electromagnet is on more than 50% of the time, the strength of the magnetic field begins to decrease, producing results below the actual condition.

In Table 3.2 below, the results of the scans of four – 3/8" strands and three – 3/8" strands are shown. The scan of four – 3/8" strands is the configuration used to represent 100% cross-sectional area of steel. The scan with three strands is a 25% reduction in strand cross-sectional area. The configuration of the three strand setup can be seen embedded in the table below. These scans were performed with the typical center-to-center distance between strands at 1.5 in. and a nominal cover (distance from sensor to strand) of 2.125 in. By looking at the results from each individual sensor and the sensors combined, detailed information about the embedded steel can be determined.

Averaging the readings from all four sensors obtains a percent area of steel over the scan width of 74%, 1% from the actual value of 75%. Looking at each sensor individually shows the condition of steel in each sensor's effect scan width. Sensor's 1, 2, and 3 are located between the missing strand and adjacent strands (denoted with the x in the image), and have values of 75% or less. Sensor 3 was most effected by removing the

strand and resulted in a value of 57%, indicating a 43% loss of cross-sectional area in its scan width. Sensor 4 is positioned the farthest from the missing strand and has the highest percentage area of steel in its effective sensor width of 81%. This test shows the area of steel within a scan width can be measured accurately and more details as to the location of the reduced cross-section can be obtained by examining individual sensor results. This test helps to understand in greater detail the effect caused by differing strand patterns. Initial lab tests were unclear on the effect of adjacent strands.

Table 3.2: Scan data for 4-strands and 3-strand arrangement. Note: In figure of strand/sensor layout, circle represents strand, x represents no strand. S1 and S2 are in same position, but on different pole faces. Complete data in Appendix C.

4 Strands							
4 Strands							
Sensor #	Max Value (G)	Min Value (G)	Scan Value (G)	Diff of Max Value - Min Value (G)	Diff of Scan Value - Min Value (G)	Area Steel (%)	
S1	1340	1162	1340	178	178	1.00	
S2	1460	1262	1460	198	198	1.00	
S3	1720	1535	1720	185	185	1.00	
S4	1705	1520	1705	185	185	1.00	
						4.00	
						% Steel / Scan Area	1.00
3 Strands							
3 Strands							
S1	1340	1162	1305	178	143	0.80	
S2	1460	1262	1415	198	153	0.77	
S3	1720	1535	1640	185	105	0.57	
S4	1705	1520	1670	185	150	0.81	
						2.95	
						% Steel / Scan Area	0.74

Chapter 4

Field Test

As part of the goal of providing ODOT with a viable inspection technology for prestressed box beams, the research team at The University of Toledo contacted Dr. Ghorbanpoor about his MFL system. He agreed to participate in the scheduled field test on a prestressed box beam in Washington Courthouse, Ohio. Including MFL in the scan allowed the author to obtain first-hand experience with the MFL technology. Performing the field test with two separate systems allowed for a comparison of the systems. Having another experienced researcher on board also helped to accelerate the advancements of the magnetic inspection technology as a whole.

A field test was performed utilizing the IMF method as well as another magnetic NDE method, Magnetic Flux Leakage (MFL), on a bridge on Washington Waterloo Road in Washington Courthouse, Ohio. The bridge was a box beam bridge consisting of two spans of nine adjacent box beams (see Figure 4-1 and Appendix A). Fayette County graciously supplied the bridge to the research team (which was scheduled for replacement), and ODOT and the Fayette County Engineer provided assistance when required. In conjunction with this research work, a team from Ohio University and the University of Cincinnati instrumented and tested this bridge to destruction. The bridge

was being replaced, which was critical to the field test because it allowed for dissection, extraction, and inspection of the embedded strands after the field test was complete. The field test was vital to the development of the test system as it required addressing all the factors important to the practical application of the test methods. Factors such as attaching the test rig to the beams, determining unknowns like actual strand position, and performing the scan in a time and cost efficient manner. The development of the practical application of the testing system is very important for this technology to be utilized by bridge inspectors and allow it to make a positive impact in society.

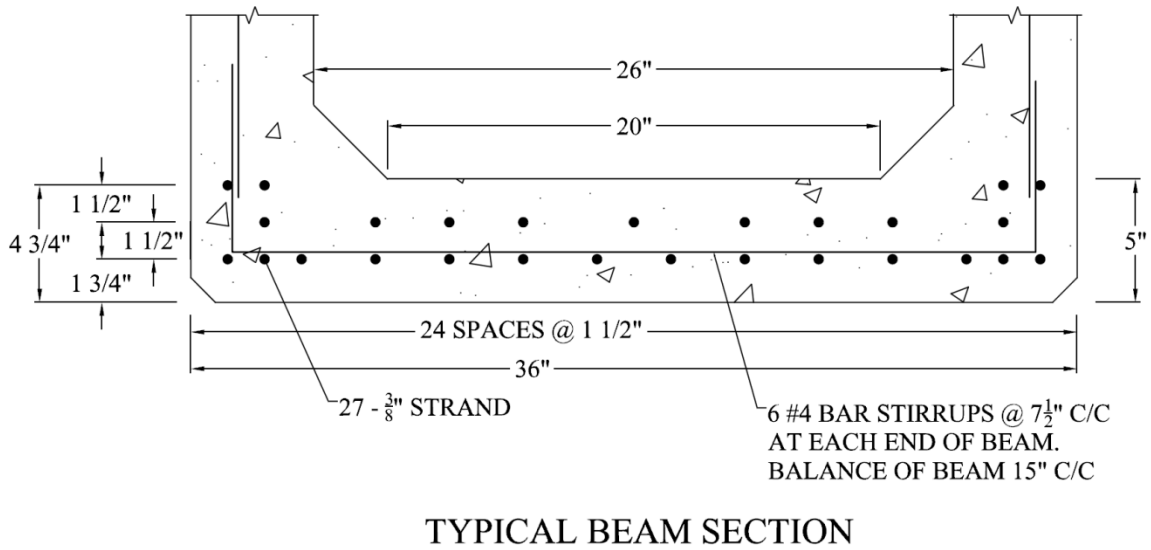


Figure 4-1: Cross section of Washington Waterloo Rd Bridge box girder (Wagner, circa 1967).

4.1 Magnetic Flux Leakage Test Setup

For the MFL system, the primary component of the system is a modular unit called the sensing head that is comprised of two permanent magnets and a series of Hall effect sensors housed in a protective box between the magnets. The inspection is performed by moving the sensing head along the bottom of the beam. The magnet induces a flux in the strands positioned above it while scanning under the bridge, and the Hall sensors simultaneously measure magnetic leakage flux. This information is acquired by a data acquisition system and recorded in a computer where it can be analyzed for magnetic leakage field. The process of scanning and recording the data is simultaneous, and can be observed on the computer as the scan is performed. Monitoring the scans in real time can indicate when a re-scan is necessary.

4.2 Field Test Platform

IMF and MFL work by running the test system under the bottom surface of the bridge box beams. The distance from the sensor to the surface of the bridge (and the embedded strand inside) must remain as consistent as possible to produce accurate test results. This presents a serious logistical issue of securing the test system to the bottom of the bridge. The IMF test equipment weighs roughly 250 pounds, making it very cumbersome to maneuver and hold in place.



Figure 4-2: Testing platform attached to bottom of bridge.

A scaffold like system was developed that attaches to the underside of the bridge using the weep holes in the bottom of the box beams (see Figure 4-2). Threaded rods with toggle bolts screwed on were inserted into the weep holes. Attachment using the weep holes is important, because it allows for quick installation and more importantly, does not damage the bridge itself. The toggle bolts expanded when inside the hollow section of the box beams and provided sufficient load capacity with easy installation. Aluminum angle was then bolted to the threaded rod. Two nuts were used on each connection to allow the angle to be adjusted vertically and locked in place. The angle served as the cross members for the platform system, and then wooden tracks were placed on top of the angles. Two people were able to install the entire setup in the field in a few hours, with another few hours of shop work previously performed.

This setup was easy to install in this situation because the portion of the bridge tested was 7 ft. above flat graded ground. In most scenarios the bridge will be over a water crossing, rough terrain, or a road/rail-way. This makes for a much more difficult situation for installing the test platform and performing the testing procedure. Lifts

and/or a snoop truck would be required to access the underside of the bridge. Reducing the weight of the system is critical in easing the testing procedure. Commercial options for under bridge scaffolding, such as Safespan, are available to provide a safe working surface for the testing. These systems can be costly and time consuming to install, but in the appropriate instances they may be the most cost effective solution.

4.3 Basic Field Test Procedure

Both magnetic systems have similar test procedures. For IMF, the scanning head includes the electromagnet and four hall sensors attached to the magnet pole faces (see Figure 4-3). For MFL the scanning head includes two permanent magnets and an array of hall sensors positioned between the two magnets (see Figure 4-4). Both systems utilized carts developed specifically for this test to fit and roll along the wooden platform. Once positioned on the platform the systems were manually rolled the length of the platform. As they were rolled the hall sensors collected information that was fed to data acquisition systems. The data acquisition systems were connected to laptop computers which processed the data and allowed for real-time viewing of the scans. This is an important feature as it indicates when a re-scan is desired. In order to make multiple passes with the scan equipment, the wooden tracks were moved horizontally on the angle in between scans. Aligning the wooden tracks with the desired test tracks proved tedious with the heavy weight of the magnets in tow. Future test rigging should address this issue and allow for less work in between scans.



Figure 4-3: IMF sensing equipment, electromagnet with hall sensors on pole face.



Figure 4-4: MFL sensing equipment.

4.4 Induced Magnetic Field Test Details and Results

IMF was the second NDE method utilized during the inspection. Due to time constraints, it was decided to investigate two tracks in the interior region, Tracks 3I and 7I (see map in Figure 4-10). These tracks were chosen because Track 3I had visible signs

of corrosion and spalling towards the end of the pier, while Track 7I had no visible signs of corrosion but the MFL scan had indicated moderate corrosion. Choosing tracks with different corrosion characteristics allowed for the best use of the limited testing time.

The tracks scanned, 3I and 7I on beam 3, were scanned along a length of approximately 12 ft. In order to estimate the cross-sectional area of the strand from the induced magnetic field values measured, data from lab experiments was utilized. In the bridge tested, the strands closest to the bottom of the box beam were embedded 1.75 in. deep inside the beam, according to the original bridge design drawing (see Figure 4-1). During testing, a gap ranging from 0.5 – 0.75 in. was maintained between the pole face and the concrete surface being scanned in order to avoid damage to the sensors fixed on the pole face. Thus, the average estimated gap between the sensors and the strand is 2 – 2.25 in. The magnetic field induced in the strand is very sensitive to the distance between the strand and the sensor. It was assumed the strands inside the box beams were at a constant distance from the magnet pole face. However, the natural deflection of the beam and the unknown of the actual cover between strand and pole face could lead to inaccuracies in the test results. There were uncertainties in the estimate of the healthy cross-section area for the strand due to the uncertainty in the distance between the strand and the sensor on the electromagnet. Another uncertainty in the test data is ultimate magnet strength. The electromagnet used in the test varies in strength as the magnet heats up with use. An estimation of the ultimate strength of the magnet was made to obtain these results. In the future, a thermocouple should be used to monitor temperature of the scans, which can be used to determine the ultimate strength of the magnet for specific test scans.

Figure 4-5 shows the magnetic field values for a laboratory test replicating the IMF scans for track 3I and track 7I. This laboratory test utilized prestressing strand magnetized using the same electromagnet used in the field test, held at a constant distance of 2.2 in. from the sensor. The graphs show the healthy value of gauss ($B_{healthy}$) for tracks 3I and 7I as well as the baseline value with the electromagnet on and no steel present (B_0). The values from Figure 4-5 were obtained using the same wooden beam that is discussed previously in Chapter 3. In order to determine the percentage corrosion for the scanned width, the values obtained from the field test (B_{corr}) are determined (see Figure 4-6). The following equation is then performed. Note: this process is the same as the test process validated in “3.2.1 Wooden Beam – Test Procedure”.

$$\text{Percentage loss} = \left(1 - \frac{(B_{corr} - B_0)}{(B_{healthy} - B_0)} \right) \times 100$$

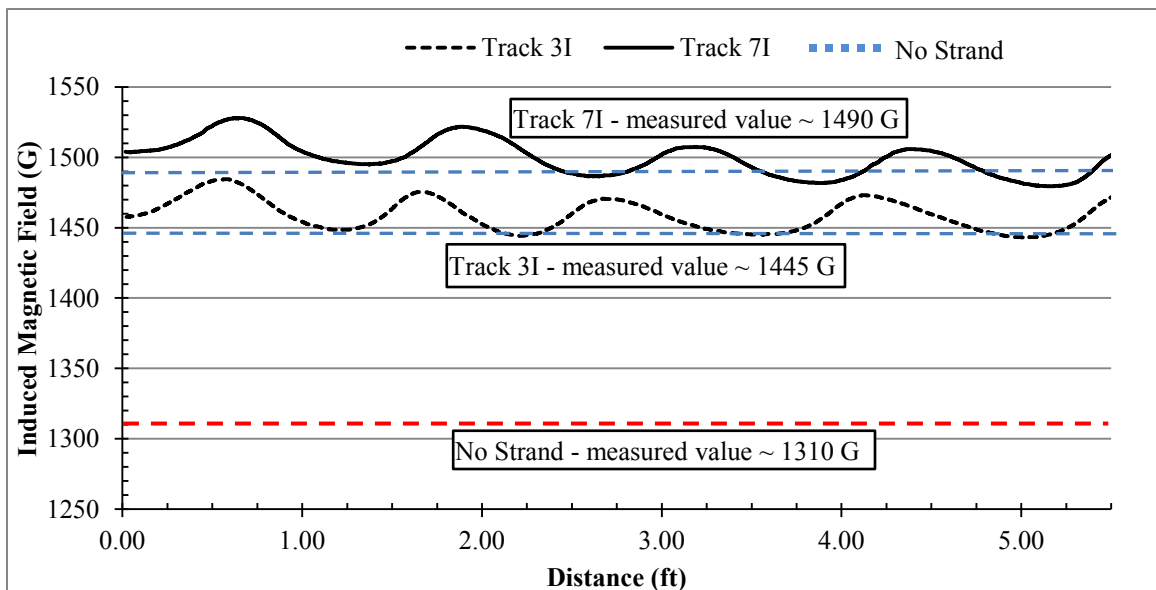


Figure 4-5: Laboratory test results for Tracks 3I and 7I setups maintained constant at 2.2 in. between pole face and strand (Fernandes, 2011).

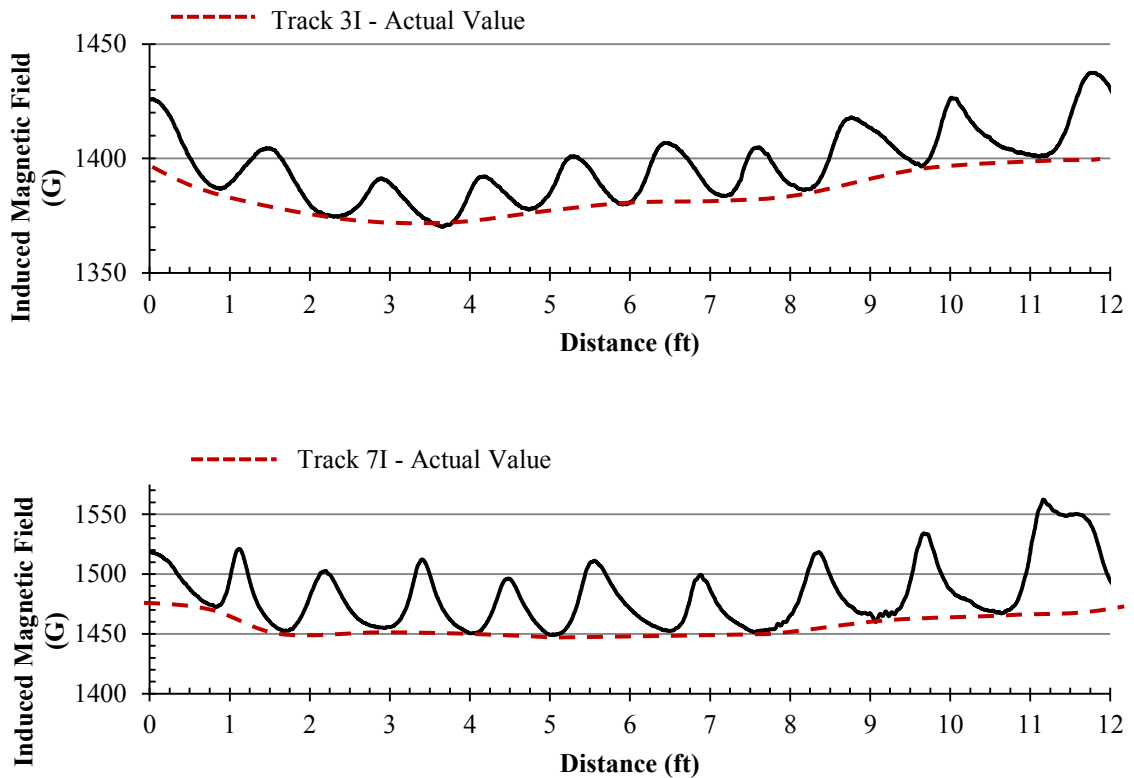


Figure 4-6: IMF scan data for interior beams – Tracks 3I and 7I.

Table 4.1 below shows the percent corrosion for the scans at regular intervals for scan 3I and 7I. The results obtained are based on two assumptions; the ultimate strength of the magnet at the time of the test scan and the actual distance from strand to sensor. These variables can have a large effect on the results obtained from the IMF scans. As previously discussed, the ultimate strength of the magnet can be documented by installing a thermocouple of the electromagnet. For this test, lab experimentation was used to estimate the ultimate magnet strength at the time of the field tests. In order to accurately assess the distance from strand to sensor, a procedure must be developed. That said, the results from the test were not accurate over the entire length of the scan, but they did

indicate corrosion. The results were accurate for the last few feet of the scan. The author believes that over this range, the distance from sensor to strand was 2.2 in., and the strand was farther from the sensor for the rest of the scan (where higher corrosion than actually found was indicated). This hypothesis cannot be verified. Overall, the IMF field test indicated corrosion, but more updated field tests are necessary to determine with confidence the accuracy of the test system.

Table 4.1. Corrosion estimated for Tracks 3I and 7I from IMF method.

Distance (ft)	Corrosion (%)	
	Track 3I	Track 7I
1	44	6
2	50	19
3	54	18
4	54	19
5	50	19
6	46	19
7	44	19
8	42	17
9	39	12
10	35	10
11	31	7
12	27	3

4.5 Magnetic Flux Leakage Test Details and Results

Each MFL test on the interior girders was approximately 12.5 ft. long and started at a position 15.75 ft. to the east of the face of the interior pier cap. On the exterior beam, each MFL test was approximately 9 ft. long and started at a position 15.5 ft. to the west of the face of the abutment located at the east side of the bridge. Each MFL test is identified with data for a specific track which covers an area with a scan width of 8 in.

and a scan length indicated for the interior and exterior beams. Locations of the MFL tracks can be seen in Figure 4-10. Each scan width of 8 in. covers multiple strands per scan. The corrosion seen in the scans are assumed to be consistent over the entire scan width. In other words, there is a certain percentage of strand area loss in the strands over the 8 in. scan width. All MFL tests were performed by supporting the MFL equipment on the temporary wooden platform and manually rolling the equipment on a set of wheels over the platform along the underside of the box beams. The weight of the MFL equipment supported by the platform was roughly 50 lbs. The underside of each selected box beam was scanned with the MFL equipment along the identified test tracks. The start and end points for all tests were marked on the underside of the box-beams to be used later during dissection.

The following results were obtained for the MFL tests performed during this investigation.

4.5.1 Interior Beams

Figure 4-7 shows MFL data for a single sensor (sensor 4 which is located at the center of the scan width) for Tracks 1I, 3I, 7I and 10I in the interior beams. The graph is a plot of magnetic leakage field (in terms of Hall sensor output voltage) as detected along the length of the track scanned. The shape and roughness of the wave form correspond to the characteristics of the strands within the track scanned. The peaks in the graph indicate the presence of transverse stirrups along the beam. The peak-to-peak width of the signal indicates the stirrup spacing in the box-beam. Indications of irregular spacing of stirrups can also be seen for Track 10I in the figure at the beginning of the test scan

(the first 3 ft.). The signal variations between peaks indicate the level of corrosion along the prestressing strand indicated in the figure. The evidence of strand fracture, or abrupt change, at the location of 9 ft. can be seen for Track 3I as an abrupt interruption in the signal. It can also be noted that the decreasing nature of peak-to-peak signal amplitude indicates the increasing depth of steel inside the concrete.

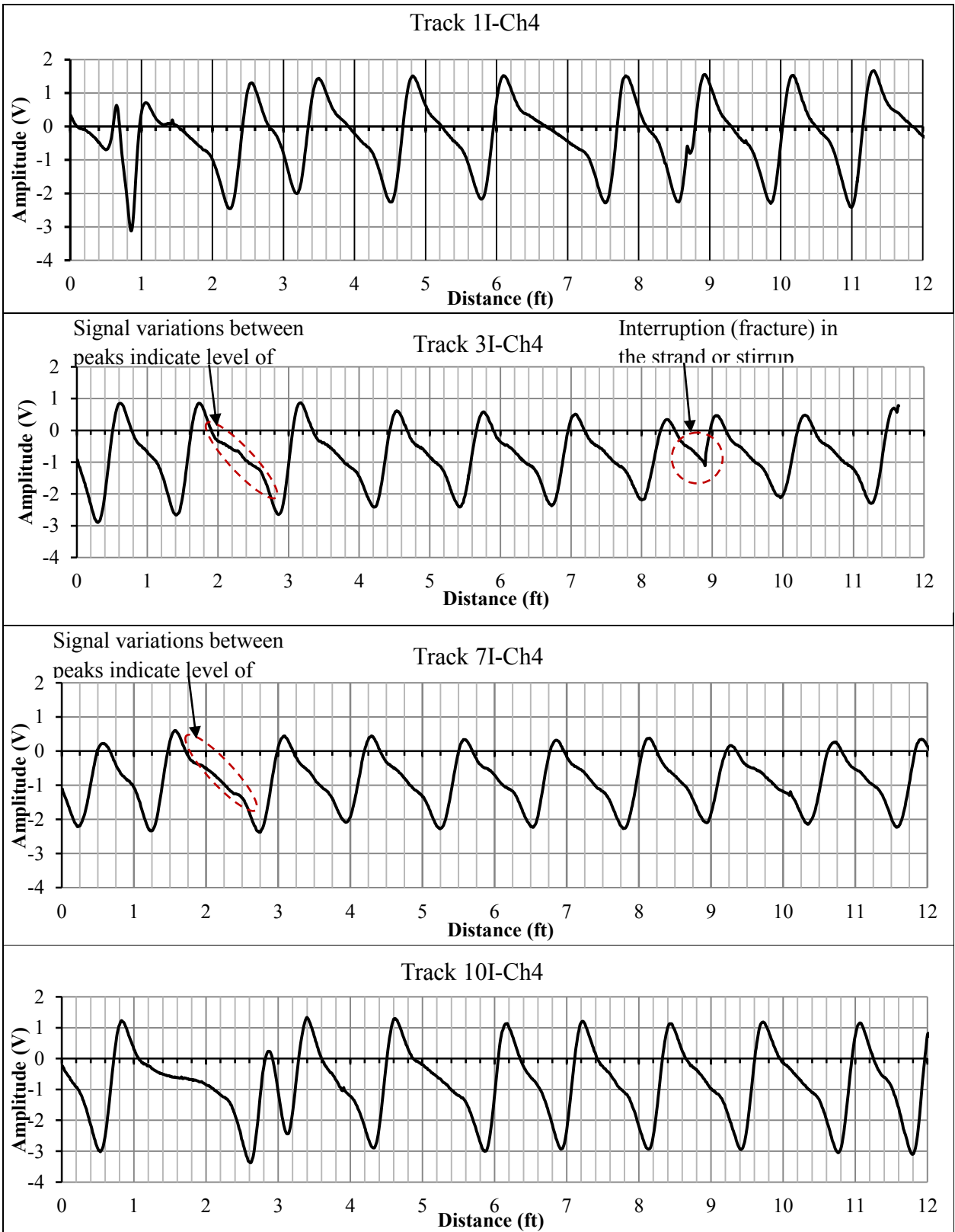


Figure 4-7: MFL scan data for interior beams – Tracks 1I, 3I, 7I and 10I.

4.5.2 Exterior Beam

Figure 4-8 shows MFL data for Tracks 1E and 3E from sensor 4 which is located at the center of the scan width. For Track 4E, the data is displayed from sensors 4 and 7 where sensor 7 is located at the north edge (at the outside edge of the beam) of the scan width. Clear indications of the presence of steel chairs as well as exposed and bent strands are shown in the data from different tracks as marked in Figure 4-8. The bumps or bends in the signal between the peaks indicate the presence of chairs at that point inside the box beam. Points of corrosion are indicated by uneven signal amplitude between peaks of the signal. The estimate of corrosion is made by zooming in on the magnetic field signal and making a correlation to the existing laboratory measurements. This method for determining the corrosion is qualitative and provides estimates of corrosion in ranges, (e.g. 10%-15%). While this estimate is not precise, it is sufficient to allow DOT officials to accurately assess the condition of the box beams in a bridge.

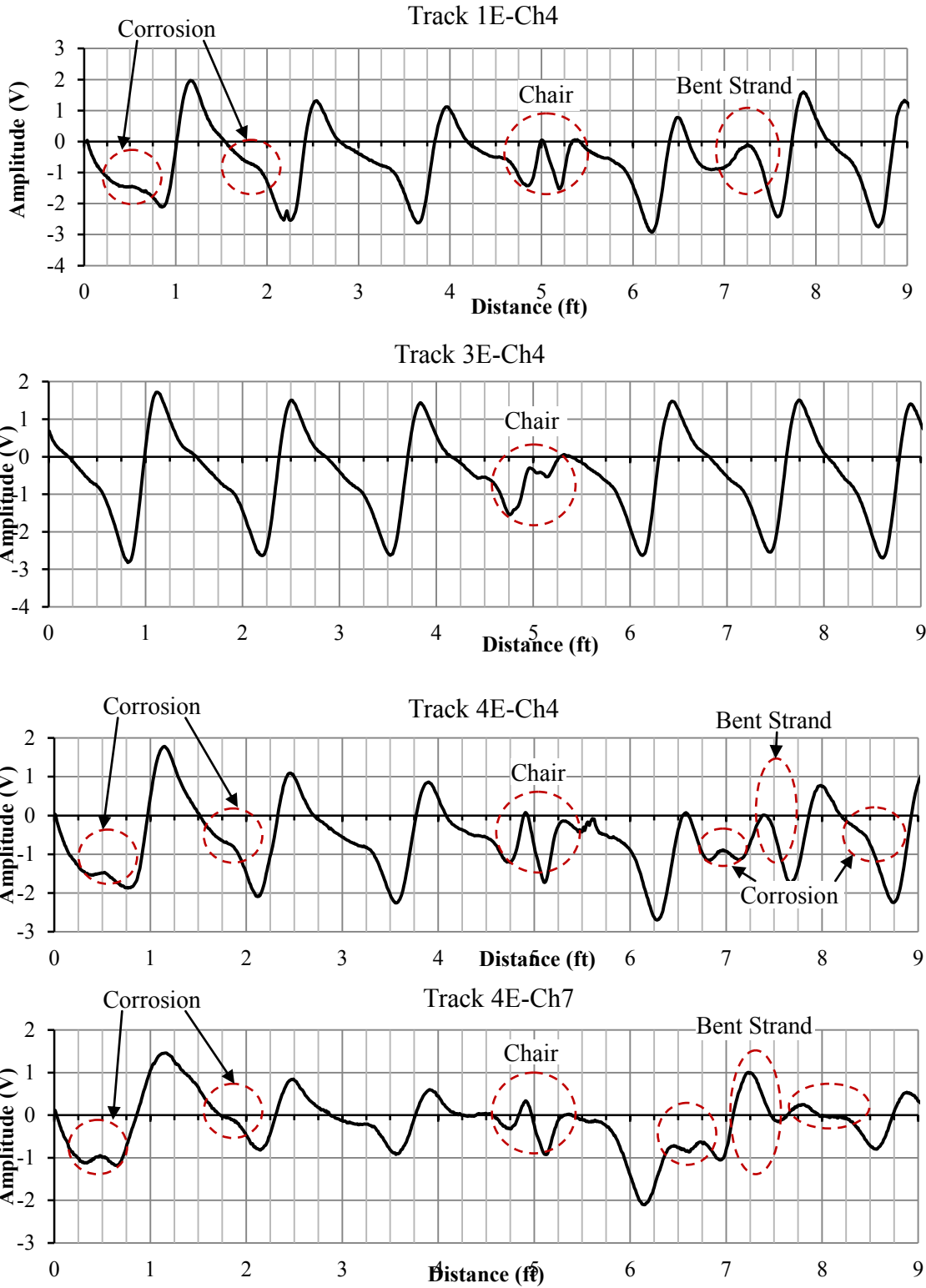


Figure 4-8: MFL scan data for exterior beams – Tracks 1E, 3E, and 4E.

4.6 Dissection and Results Comparison

After the field tests were completed the bridge was dissected in the portions tested, these areas are shown as the interior and exterior regions of Figure 4-10. Concrete was chipped away to expose the bottom layer of strands. The strands were then extracted from the bridge to be analyzed in the lab. Due to the difficulty of exposing strands, specific areas of interest were selected based upon visual and NDE (MFL & IMF) inspection results. The dissections were necessary in order to determine the accuracy of the test results. After dissection was completed and the strands had been extracted from the beams, the strands were visually measured and examined in the lab to determine their level of corrosion. Observations are in Table 4.1. Visual inspection of the strand was performed after loose rust was mechanically removed. The strands were then cut to expose the cross-section (see Figure 4-9). The black lines on figure 4-10 shows the locations of the test track, and the red boxes represent areas of corrosion detected by the MFL inspection. Specific details of the corrosion are written in red letters above the red boxes that indicate corrosion. Figure 4-10 also shows the dissection locations (numbers encapsulated in black circles).



Figure 4-9: Cut strand cross-section (in.) (Track 3I – Dissection Area 2).

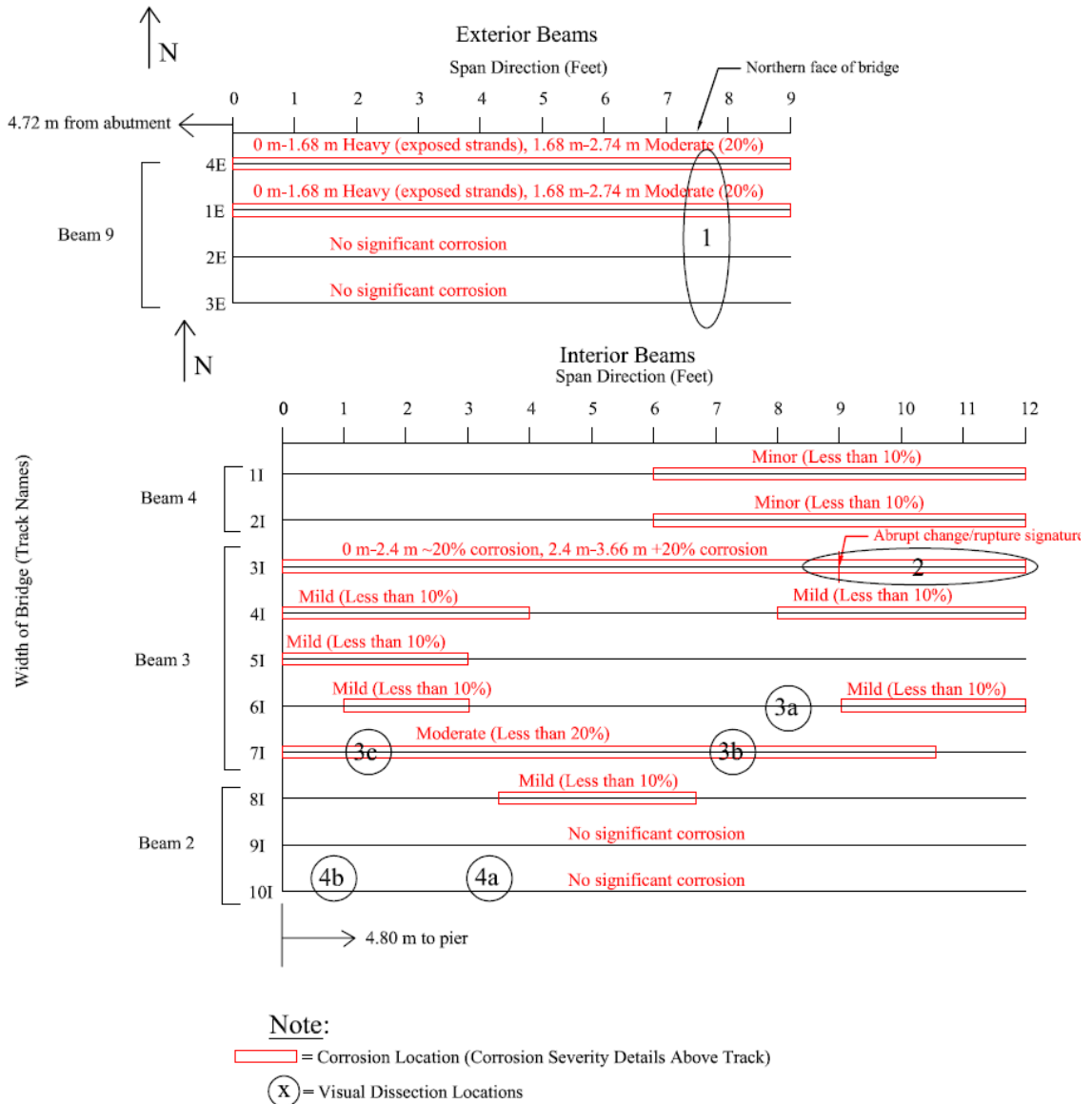


Figure 4-10: Results for corrosion detected for interior and exterior tracks by MFL method – reflected plan.

The results in Table 4.1 for MFL show an accurate correlation between the test results and actual condition of the strand for a majority of the scan tracks. MFL indicated moderate corrosion (20%) in Track 7I, but upon dissection, little corrosion was found in the strands. While the inaccuracy is not desirable it was a false positive, meaning bridge inspectors would be erring conservatively as opposed to the more dangerous situation of not finding corrosion in a damaged strand.

The MFL testing predicted medium to heavy corrosion in dissection area 2 of beam 3, which can be seen in Figure 4-11. The strands from 8 – 10 in., which were completely or partially exposed, show heavy corrosion. The previously embedded strands, from 4 – 7 in., show corrosion that gets progressively lighter as the distance from the joint increases. The magnetic testing was accurate in this region, except that we were unable to find a full break in strands during dissection as depicted in the MFL scan.



Figure 4-11: Dissection results of Area 2 in interior beam 3.

The results from the IMF test indicated corrosion in the prestressing strand. When compared with the dissection findings, the IMF method needs to improve accuracy. For the reasons stated previously (unknown distance from strand to sensor and

uncertainty in ultimate magnetic strength) the results did not correlate well with the dissection findings. In order to obtain a truly accurate reading, the distance between strands and sensor face must be known. In the future this issue must be addressed; commercial methods have been identified as possible solutions, such as the Proceq Profometer 5+. A thermocouple should also be installed which can measure temperature, which can be correlated to ultimate magnetic strength.

Table 4.2: Results obtained from dissection of bridge compared with MFL and IMF estimated corrosion results over entire scan length (Note: --- indicates no inspection performed).

Track I.D.	MFL method (% corrosion)	IMF method (% corrosion)	Actual Strand Condition (% corrosion)
Interior Beams			
1I	<<10%	---	---
2I	<<10%	---	---
3I	~20%	27% - 54%	10% - 30%
4I	<10%	---	5%
5I	<10%	---	---
6I	<10%	---	No significant corrosion
7I	<20%	3% - 19%	No significant corrosion
8I	<10%	---	---
9I	No significant corrosion	---	No significant corrosion
10I	No significant corrosion	---	No significant corrosion
Exterior Beams			
4E	~20%	---	20%
1E	~20%	---	15%-20%
2E	<10%	---	10%-15%
3E	No significant corrosion	---	5%

Chapter 5

Bridge Inspection

Magnetic inspection coupled with the guidelines recommended by the Lehigh report discussed earlier could provide a more complete inspection system for prestressed box beams. Improving the inspection process would help insure DOT funds go to the appropriate bridges and that bridges remain safe for the public.

5.1 Inspection Recommendations

An annual visual bridge inspection is important to assessing a bridges condition. Crack logs/maps documenting the location and size of cracks can provide indications towards the condition of a bridge and its progression. The flowchart below includes information about corrosion that corresponds to longitudinal cracking, (see Figure 5-1) (Naito, et. al, 2010). When a certain level of longitudinal cracking is found, determined by DOT officials, it would be beneficial to utilize magnetic NDE methods to obtain more details on the condition of the embedded strand. Other factors besides longitudinal cracking may go into the decision to use magnetic methods. Bridge value, location, and traffic density can also affect the decision making process.

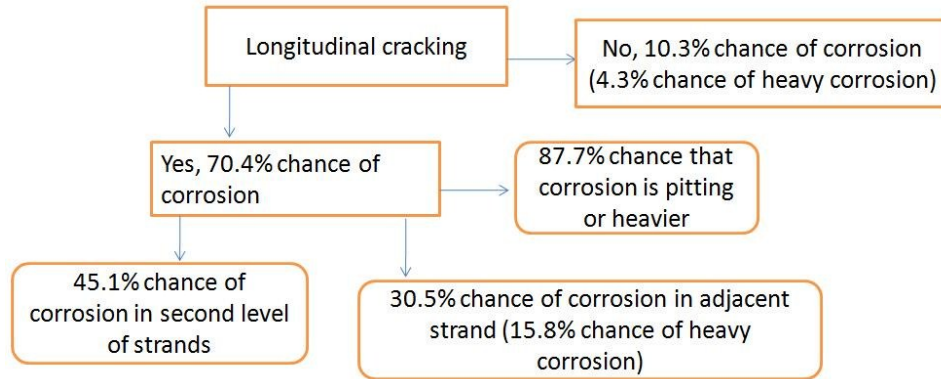


Figure 5-1: Inspection flowchart, longitudinal crack patterns. Data from (Naito, et al. 2010).

The corrosion data obtained from magnetic NDE methods is valuable. Knowing the relative strength of embedded strand with certain cross-sectional losses takes the information a step further. In 2006 Naito, et. al, performed an in depth study on the embedded strand from the box beams of the Lake View Drive Bridge over I-70. This study involved testing strands with various level of corrosion to determine the relative strength. The data from this study is summarized in Table 5.1 below. Figure 5-2, also from a Naito report, shows examples of the different levels of corrosion. The results of IMF and MFL coupled with this data can be used to perform load ratings of bridges.

Table 5.1: Strength of corroded strand, (Naito, et al 2006).

Average Wire Strength Due to Corrosion		
Wire Condition:	Strength (ksi)	Relative Strength
Light Corrosion (No Section Loss)	288.0	100%
Pitting (10% Section Loss)	230.0	79.9%
Heavy Pitting (20% Section Loss)	205.6	71.4%

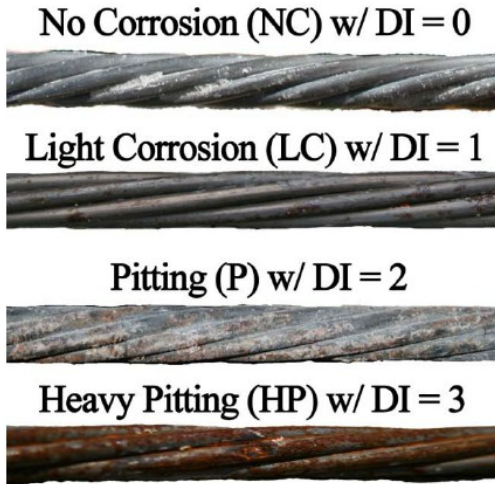


Figure 5-2: Corrosion levels on strand (Naito, et. al, 2010).

5.2 Maintenance and Repair

Maintenance should be performed during each inspection to ensure that the beam weep holes are open and free of debris to allow water to drain from the beams. Many box beams of this era were constructed with vent holes on the top of the beams to allow heat to escape during the curing process and weep holes on the bottom of the beam to allow any water collected to run out. After curing is finished the vent holes should have been blocked off while the weep holes should remain clear and open to allow any moisture to escape the beams. In many instances, the vents were left open and water, often times containing chloride, was trapped in the hollow sections of the box beams because the weep holes were either never opened or blocked by cardboard forming materials, and allowed to attack the concrete (Naito, et al., 2010). The weep holes on the beams from the Washington Waterloo Road Bridge were closed and when opened for the installation of our test system a great deal of water was released. Furthermore, when the

bridge was eventually tested to destruction by the researchers from OU and UC, water poured from the beams as cracks formed on the bottom of the beams. This water is detrimental to the beams as it adds dead load to the bridge and can deteriorate the concrete through the chloride present and the freeze-thaw cycle. In box beam bridge inspection, it is essential that the weep holes are checked to ensure they remain open, clear of debris, and functional.

Other maintenance steps can be taken to prolong the life of box beam bridges. A survey conducted by Precast/Prestressed Concrete Institute (PCI) of the states who utilize box beam bridges highlighted the following maintenance and repair tasks to extend useful life. Sealing the deck, removing the asphalt topping, sealing cracks, and washing the deck annually can extend the life of box beams (Russell, 2011). These tasks focus on preventing water, especially water contaminated with chlorides, from getting into the joints between the box beams and into the beams themselves. This contaminated water can degrade the concrete and cause early bridge failure. The following repair procedures were also recommended; adding a reinforced concrete deck, supplemental tie rods, replacing the asphalt wearing surface with a concrete deck, and using waterproofing membrane over the entire surface of the deck (Russell, 2011). These procedures also prevent water from entering the bridge structure and the tie rods ensure that the box beams are connected and act as one member when a load is applied.

Chapter 6

Conclusions and Future Work

Laboratory and field test data has been presented of an induced magnetic field nondestructive evaluation technique. Magnetic flux leakage was also utilized in the field test. The field test involved testing a bridge using these NDE systems, and dissection and extraction of strands to verify results. The results were desirable in most instances, but hurdles to implementing the technology were uncovered. The ability to access the underside of a bridge with the equipment, the variability of the strand position within the beams, and the consistent accuracy of the test systems must be further researched.

6.1 Conclusions

This thesis furthered development of the IMF technology through laboratory and field testing. The research identifies two technologies as a possibility for providing ODOT with a successful NDE technology for prestressed box beams, IMF and MFL. The MFL system is a possible candidate for a NDE system for prestressed box beams. It has been used to determine corrosion in a variety of settings and has proven accurate in testing box beams. The MFL system provides qualitative data of corrosion and the results must be determined from graphs by an individual trained to identify flaws in the

graphs. While the IMF system is younger in development, laboratory tests have shown that it can be accurate within +/- 7%, while providing more quantitative data than MFL's ranges of corrosion. Optimization of the test process and an improved magnet design would improve this accuracy. Currently, the electromagnet has varying strength dependent on the length of time it is on during a testing session. If the electromagnet is on for too long, magnetic strength decreases, which disturbs the accuracy of the test method. A thermocouple monitoring heat, which is related to ultimate strength, could be used to solve this issue. Permanent magnets may be more appropriate because they would have steadier magnetic strengths during a test session. Another challenge with the IMF electromagnet is its weight of 250 lbs., this must be reduced or a more elegant test platform must be devised. Regardless of the test technology utilized, magnetic inspection technologies of prestressed box beams have shown promise.

6.2 Improvements and Future Work

In order to make magnetic detection a reliable tool for prestressed box beam bridge inspection it must be proved accurate in a variety of settings and tests. The University of Toledo has proposed a more detailed study of MFL by performing tests on aged box beams that have been extracted from bridges. These beams would be set upside down to allow for easy testing. The ease of testing would allow for a focus on the magnetic method itself, not the difficulty in suspending the system from bridges. The difficulty of suspending the magnetic test systems is a large hurdle to overcome.

To improve upon the IMF method, two obstacles must be solved to ensure accuracy. First, a thermocouple should be installed that will monitor temperature,

therefore ultimate magnetic strength, during test scans. If this method is unsuccessful, it is possible that permanent magnets could be used in place of the electromagnet.

Secondly, a method to determine the distance from sensor (magnet pole face) to strand must be developed. This method needs to be function when strand is embedded in concrete and its position is unknown. Solving these two problems would allow for the IMF system to be reliable and accurate for testing corrosion in the prestressing strand in prestressed box beams.

A cost effective solution must be developed to solve the issue of testing on the underside of bridges. In order to obtain accurate test results the NDE systems must run smoothly under the bridges suspended at a relatively stable distance from the beam throughout the scan. This makes snoopers less than ideal as a base for the test. More likely would be the use of a snoopers to construct a test platform on the bridge. This platform could be constructed from aluminum that is lightweight, nonmagnetic, and strong. Tests could then be conducted with the inspectors operating out of the snoopers. Other methods for suspending the system have been discussed, such as a series of high tensioned cables holding the sensing system that could allow access to the entire underside of a bridge, similar to Skycam used for filming professional sporting events. Remote control operation of this device, or any device similar, would keep inspectors in a safe position and allow for an efficient inspection process.

References

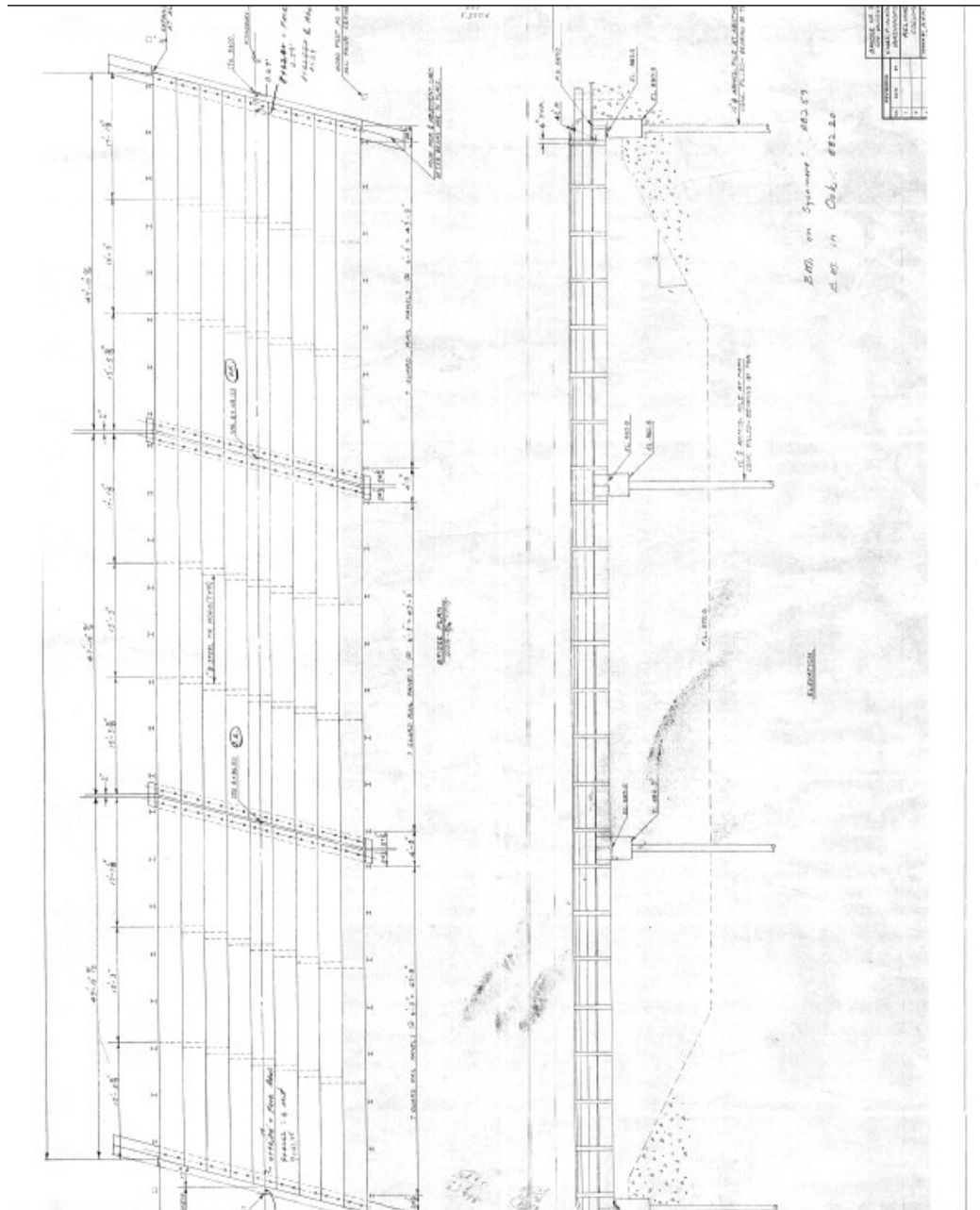
- “Standard Practice for Electromagnetic Examination of Ferromagnetic Steel Wire Rope.” ASTM E1571, American Society for Testing Materials, 2007.
- Chen, L., Que, P. W., and Jin, T. (2005). “A Giant-Magneto-resistance Sensor for Magnetic-Flux-Leakage Nondestructive Testing of a Pipeline.” *Russian Journal of Nondestructive Testing*, 41(7), 462-465.
- Ciolko, A. T. and Tabatabai, H. (1999). “Nondestructive Methods for Condition Evaluation of Prestressing Steel Strands in Concrete Bridges.” *Final Report: Phase I - Technology Review*, National Cooperative Highway Research Program, Transportation Research Board, Washington, DC.
- DaSilva, M, Javidi, S., Yakel, A. and Azizinamini, A. (2009). “Nondestructive Method to Detect Corrosion of Steel Elements in Concrete.” *Final Report NDOR Research Project No. P597*, National Bridge Research Organization, University of Nebraska-Lincoln and The Nebraska Department of Roads.
- Edwards, M. A. (1999). “Nondestructive evaluation of concrete structures based on magnetic flux leakage concepts.” M.S. Thesis, The University of Wisconsin-Milwaukee, Milwaukee, WI.
- Fernandes, B. (2010). “Nondestructive Evaluation of Deteriorated Prestressing Strands Using Magnetic Field Induction.” M.S. Thesis, The University of Toledo, Toledo, OH.
- Fernandes, B., Wade, J., Nims, D. and Devabhaktuni, V. (2010). “Development of a Sensor for Nondestructive Inspection of Deteriorated Prestressing Strands in Prestressed Concrete Bridges,” *NDE/NDT for Highways and Bridges: Structural Materials Technology Conference*, ASNT, New York City, NY, 162-170.
- Fernandes, B., Titus, M., Nims, D., Devabhaktuni, V, (2011). “A Field Test of Magnetic Methods for Corrosion Detection in Prestressing Strands in Adjacent Box Beam Bridges.” Article in preparation for submission to ASCE Bridge Journal.

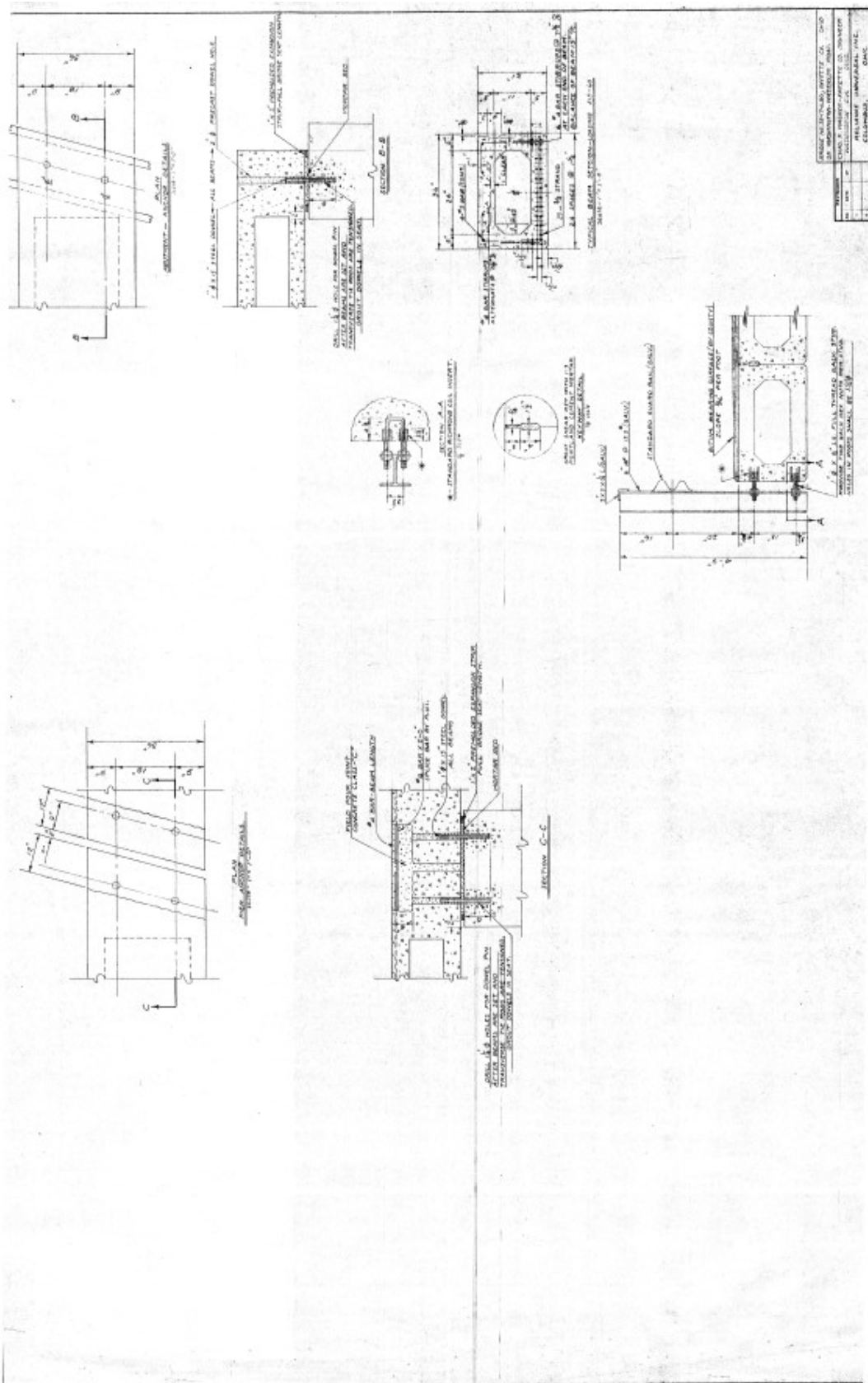
- Ghorbanpoor, A. (1998a). "Magnetic Flux Leakage NDE of Concrete Bridges." *The Proceedings of the 77th Annual Meeting of the Transportation Research Board*, Washington, D.C.
- Ghorbanpoor, A. (1998b). "Magnetic-Based NDE of Steel in Prestressed and Post-Tensioned concrete Bridges," *The Proceedings of the 1998 Structural Materials Technology Non-Destructive Testing Conference*, San Antonio, TX.
- Ghorbanpoor, A. (2000). "Condition Assessment of External P-T Tendons in the Mid-Bay Bridge," *Final Report*, Florida Department of Transportation, Tallahassee, FL.
- Ghorbanpoor, A., Borchelt, R., Edwards, M., and Abdel Salam, E. (2000). "Magnetic-Based NDE of Prestressed and Post-Tensioned Concrete Members – The MFL System." *Final Report FHWA-RD-00-026*, Federal Highway Administration, US Department of Transportation, McLean, VA.
- Ghorbanpoor, A. (2010). "MFL Tests at P/S Concrete Box Girder Bridge." *Summary Report*, submitted to Dr. Douglas Nims of University of Toledo.
- Hillemeier, B. and Scheel, H. (1998). "Magnetic Detection of Prestressing Steel Fractures in Prestressed Concrete." *Materials and Corrosion*, 49, 799-804.
- Jones, L., Pessiki, S., Naito, C. and Hodgson, I. (2010). "Inspection methods & techniques to determine non visible corrosion of prestressing strands in concrete bridge components, Task 2 – Assessment of candidate NDT methods." *ATLSS Report No. 09-09*, Lehigh University, Bethlehem, PA and Pennsylvania Department of Transportation, Harrisburg, PA.
- Kusenberger, F. N. and Barton, J. R. (1981). "Detection of Flaws in Reinforcement Steels in Prestressed Concrete Bridges." *Final Report FH-WA/RD-81/087*, Federal Highway Administration, Washington, DC.
- Mihalache, O., Preda, G., Yusa, N. and Miya, K. (2000). "Experimental Measurements and Numerical Simulation of OD and ID in Plate Ferromagnetic Materials Using Magnetic Flux Leakage." *Energy and Information in Non-Linear Systems, Proc. of the 4th Japan-Europe Joint Workshop*, Brno, Czech Republic, 106-109.
- Naito, C. and Warncke, J. (2008). "Inspection methods & techniques to determine non visible corrosion of prestressing strands in concrete bridge components, Task 1 – Literature Review." *ATLSS Report No. 09-10*, Lehigh University, Bethlehem, PA and Pennsylvania Department of Transportation, Harrisburg, PA.

- Naito, C. and Jones, L. (2010). "Nondestructive Inspection of Strand Corrosion in Prestressed Concrete Box Beam Members." *NDE/NDT for Highways and Bridges: Structural Materials Technology Conference*, ASNT, New York City, NY, 214-219.
- Naito, C., Jones, L., and Hodgson, I. (2010). "Inspection methods & techniques to determine non visible corrosion of prestressing strands in concrete bridge components, Task 3 – Forensic Evaluation and Rating Methodology." *ATLSS Report No. 09-10*, Lehigh University, Bethlehem, PA and Pennsylvania Department of Transportation, Harrisburg, PA.
- Naito, C., Sause, R., Hodgson, I., Pessiki, S., Desai, C., "Forensic Evaluation of Prestressed Box Beams from the Lake View Drive Bridge over I-70 – Final Report." *ATLSS Report No. 06-13 and FHWA-PA-2006-017-EMG002*, ATLSS Center, Lehigh University, September, 2006, 62 pages.
- Rumiche, F., Indacochea, J. E. and Wang, M. L. (2008). "Detection and Monitoring of Corrosion in Structural Carbon Steels Using Electromagnetic Sensors." *Journal of Engineering Materials and Technology*, 130(3), 031008.
- Russell, H., "Adjacent precast concrete box-beam bridges: State of the practice." *PCI Journal*, Winter 2011, 75-91.
- Sawade, G. and Krause, H-J. (2007). "Inspection of Prestressed Concrete Members Using the Magnetic Leakage Flux Measurement Method – Estimation of Detection Limit." *Advances in Construction Materials 2007*, Springer, Berlin, Germany, 639-649.
- Scheel, H. and Hillemeier, B. (1997). "Capacity of the Remnant Magnetism Method to Detect Fractures of Steel in Tendons Embedded in Prestressed Concrete." *NDT & E International*, 30(4), 211-216.
- Scheel, H. and Hillemeier, B. (2003). "Location of Prestressing Steel Fractures in Concrete." *Journal of Materials in Civil Engineering*, ASCE, 15(3), 228-234.
- Wade, J. (2010). "Magnetic Sensor for Nondestructive Evaluation of Deteriorated Prestressing Strand." M.S. Thesis, The University of Toledo, Toledo, Ohio.
- Wagner, C.P. (circa 1967). "Bridge No. 35-17-6.80, Fayette Co. Ohio on Washington-Waterloo Road." Office of Fayette County Engineer, Washington Courthouse, OH, 2.

Appendices

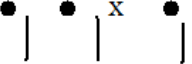
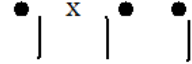
Appendix A





DESIGNED BY	ARCHITECTS
DRAWN BY	ARCHITECTS
CHECKED BY	ARCHITECTS
DATE	1954
PROJECT	RESEARCH LABORATORY, INC.
CITY	COLUMBUS, OHIO

Appendix C

							
4 Strands	S3	S1/S2	S4				
Sensor #	Max Value	Min Value	Scan Value	Diff of Max Value - Min Value	Diff of Scan Value - Min Value	% Steel	
S1	1340	1162	1340	178	178	1.00	
S2	1460	1262	1460	198	198	1.00	
S3	1720	1535	1720	185	185	1.00	
S4	1705	1520	1705	185	185	1.00	
						4.00	
						% Steel / Scan Area	1.00
							
3 Strands	S3	S1/S2	S4				
S1	1340	1162	1275	178	113	0.63	
S2	1460	1262	1400	198	138	0.70	
S3	1720	1535	1680	185	145	0.78	
S4	1705	1520	1640	185	120	0.65	
						2.76	
						% Steel / Scan Area	0.69
							
3 Strands	S3	S1/S2	S4				
S1	1340	1162	1280	178	118	0.66	
S2	1460	1262	1410	198	148	0.75	
S3	1720	1535	1670	185	135	0.73	
S4	1705	1520	1675	185	155	0.84	
						2.98	
						% Steel / Scan Area	0.74
							
3 Strands	S3	S1/S2	S4				
S1	1340	1162	1298	178	136	0.76	
S2	1460	1262	1415	198	153	0.77	
S3	1720	1535	1675	185	140	0.76	
S4	1705	1520	1610	185	90	0.49	
						2.78	
						% Steel / Scan Area	0.70

3 Strands	s3	s1/s2	s4			
S1	1340	1162	1305	178	143	0.80
S2	1460	1262	1415	198	153	0.77
S3	1720	1535	1640	185	105	0.57
S4	1705	1520	1670	185	150	0.81
					2.95	
					% Steel / Scan Area	0.74
2 Strands	s3	s1/s2	s4			
S1	1340	1162	1255	178	93	0.52
S2	1460	1262	1360	198	98	0.49
S3	1720	1535	1615	185	80	0.43
S4	1705	1520	1628	185	108	0.58
					2.03	
					% Steel / Scan Area	0.51
2 Strands	s3	s1/s2	s4			
S1	1340	1162	1240	178	78	0.44
S2	1460	1262	1348	198	86	0.43
S3	1720	1535	1635	185	100	0.54
S4	1705	1520	1625	185	105	0.57
					1.98	
					% Steel / Scan Area	0.50
2 Strands	s3	s1/s2	s4			
S1	1340	1162	1240	178	78	0.44
S2	1460	1262	1352	198	90	0.45
S3	1720	1535	1575	185	40	0.22
S4	1705	1520	1635	185	115	0.62
					1.73	
					% Steel / Scan Area	0.43
1 Strand	s3	s1/s2	s4			
S1	1340	1162	1210	178	48	0.27
S2	1460	1262	1320	198	58	0.29

S3	1720	1535	1560	185	25	0.14	
S4	1710	1520	1570	190	50	0.26	
						0.96	
						% Steel / Scan Area	0.24